Presented at the US/PRC
Flood Forecasting Symposium/Workshop
Shanghai, PRC
April 14-17, 1992

NWS RIVER MECHANICS: SOME RECENT DEVELOPMENTS[1]

by
D. L. Fread
National Weather Service (NWS)
Office of Hydrology
Hydrologic Research Laboratory, Director

ABSTRACT

Some recent developments in the NWS river mechanics area are presented. They are applicable to the NWS hydrology program for river and water resource forecasting services as well as elsewhere. First, a level-pool routing algorithm which is very efficient for computer applications is described. Also, the accuracy of reservoir level-pool routing is defined by empirical nondimensional functions of reservoir length, depth, and volume as well as the shape and volume of the inflow hydrograph. Second, a nonlinear Muskingum-Cunge diffusion-type river routing algorithm is described. Also, its error properties are defined by empirical functions of the channel slope and the hydrograph time of rise. Third, a theoretical derivation is presented for the selection criteria for the maximum size of computational distance and time step parameters for implicit dynamic routing models such as NWS DAMBRK, DWOPER, and FLDWAV. Fourth, recent improvements in the NWS Simplified Dam-Break (SMPDBK) model are described. Fifth, a physically based algorithm is derived for computing threshold runoff values, which indicate the necessary runoff to produce overbank flash flooding in small streams. The parameters in the threshold runoff algorithm are evaluated from digital terrain databases in combination with a Geographical Information System (GIS) and accompanying computer software.

1.0 Introduction

Simplified routing models have long been utilized in the National Weather Service (NWS) hydrology program for river and water resource forecasting services. Also, more sophisticated routing models based on the complete one-dimensional Saint-Venant equations of unsteady flow have been developed and are being implemented, as resources are available, for particularly complex routing applications such as dam-break floods, major river systems subject to backwater effects, and tidal estuaries. This paper presents guidance for selecting which routing applications should be considered for the Saint-Venant based dynamic routing model and which are suitable for two particular simplified routing models, i.e., (1) a simple level-pool reservoir routing model and (2) a simple diffusion-type river routing model known as the Muskingum-Cunge method. Suitability of the simplified models is assessed on the basis of the routing error as determined by the deviation of computed flows between the simplified and Saint-Venant based models.

---

[1] Presented at the US/PRC Flood Forecasting Symposium/Workshop, Shanghai, PRC, April 14-17, 1992.

A critical aspect of applying Saint-Venant based models is the selection of the computational time steps (Δt) and distance steps (Δx). A theoretical derivation is presented herein for the Δt and Δx selection criteria for implicit dynamic routing models as used in the NWS. These criteria are related to empirical criteria which have been used in the past.

The NWS Simplified Dam-Break Model provides acceptable accuracy for dam-break flood prediction in cases where the river/valley downstream of the failed dam is uncomplicated by levees, dams, lakes, estuaries, large tributaries and natural or man-made constrictions which cause significant backwater effects. This paper reviews some recent improvements in the model which corrects two modeling deficiencies for uncomplicated downstream river/valley dam-break scenarios. These deficiencies are: (1) occasional non-convergence of the iterative procedure for computing the peak discharge of the breached dam when reduction of the discharge due to submergence effects of the downstream tailwater depth is likely to occur, and (2) the lack of sufficient reduction in the flood wave celerity associated with dam-break waves propagating through downstream valleys having significant off-channel (dead) storages.

Lastly, this paper presents the derivation of a physically based algorithm for computing threshold runoff values used for flash flood guidance in the NWS. The threshold runoff indicates the necessary runoff to produce overbank flash flooding in small streams. The algorithm's parameters are restricted to those that can be automatically obtained from a Geographical Information System (GIS) along with terrain databases and minimal site observations.

2.0 Level-Pool Reservoir Routing Algorithm and Error Properties

When flood waves are routed through reservoirs, the routing algorithm normally chosen is a very simple one called "level-pool" routing. In this technique, the reservoir is assumed to always have a horizontal water surface throughout its length and throughout the time in which the flood wave moves through the reservoir. The water-surface elevation (h) changes with time (t), and the reservoir outflow (Q) is assumed to be a function of h(t) as well as any movable gate settings.

Over the years, several level-pool routing techniques have been used, all of them based on the principle of conservation of mass, i.e.,

$$\tilde{I}(t) - \tilde{Q}(t) = dS/dt \tag{2.1}$$

in which $\tilde{I}(t)$ is the average inflow over the time interval (dt), $\tilde{Q}(t)$ is the average outflow (discharge) from the reservoir over the time interval, and dS is the change in storage during the time interval. Initially, most level-pool routing techniques were graphical or semigraphical; then with the advent of computers, they were computerized utilizing table look-ups. However, since Eq. (2.1) is an ordinary differential equation, it can be solved readily by various numerical techniques.

2.1 Iterative Trapezoidal Integration Algorithm

One very efficient numerical technique developed by Fread (1977) is an iterative trapezoidal integration algorithm which integrates the conservation of mass Eq. (2.1). In this algorithm, the time domain consists of time lines separated by Δt intervals, i.e., $t=0$, Δt, $2\Delta t$, ..., $j\Delta t$, $(j+1)\Delta t$. The time rate of change in storage is the product of reservoir surface area (Sa) and change of water-surface elevation (h) over the jth time step, i.e.,

$$dS/dt = 0.5(Sa^{j} + Sa^{j+1})(h^{j+1} - h^{j})/\Delta t^{j} \tag{2.2}$$

in which the surface area (Sa) is specified as a known tabular function of h.

Using arithmetic averages for $\tilde{I}(t)$ and $\tilde{Q}(t)$ over the Δt interval and substituting Eq.(2.2) into Eq.(2.1) yields the following:

$$0.5(I^{j} + I^{j+1}) - 0.5(Q^{j} + Q^{j+1}) - 0.5(Sa^{j} + Sa^{j+1})(h^{j+1} - h^{j})/\Delta t^{j} = 0 \tag{2.3}$$

The inflow (I) at times j and j+1 are known from the specified inflow hydrograph, the outflow (Q) at time j can be computed from the known water-surface elevation (h^j), any movable gate settings, and an appropriate spillway discharge equation or rating curve. The surface area (Sa^j) can be determined from the known value of h^j. The unknowns in the equation consist of h^{j+1}, Q^{j+1}, Sa^{j+1}; the latter two are known nonlinear functions of h^{j+1}. Hence, Eq. (2.3) can be solved for h^{j+1} by an iterative method such as Newton-Raphson, i.e.,

$$h_{k+1}^{j+1} = h_k^{j+1} - f\left(h_k^{j+1}\right)/f'\left(h_k^{j+1}\right) \tag{2.4}$$

in which k is the iteration counter; and $f\left(h_k^{j+1}\right)$ is the left-hand side of Eq. (2.3) evaluated with the first estimate for h_k^{j+1}, which for $k=1$ is either h^j or a linear extrapolated estimate of h^{j+1}. Also, $f'\left(h_k^{j+1}\right)$ is the derivative of Eq. (2.3) with respect to h^{j+1}; the derivative can be approximated by using a numerical derivative as follows:

$$f'\left(h_k^{j+1}\right) = \left[f\left(h_k^{j+1} + \varepsilon\right) - f\left(h_k^{j+1} - \varepsilon\right)\right] / \left[\left(h_k^{j+1} + \varepsilon\right) - \left(h_k^{j+1} - \varepsilon\right)\right] \tag{2.5}$$

in which ε is a small value, say 0.1 ft (0.03 m). Using Eq. (2.4), only one or two iterations are usually required to solve Eq. (2.3) for h^{j+1}. Initially, the reservoir pool elevation (h^j) must be known to start the computational process. Once h^{j+1} is obtained, Q^{j+1} can be computed from the spillway discharge equation.

2.2 Error Properties of Level-Pool Routing

The assumption in the level-pool routing algorithm of a horizontal (level) water surface along the length of the reservoir at all times can cause errors in the routed (computed) discharges and water-surface elevations. The validity of this assumption depends on (1) the routing time interval, Δt (which is usually 1/7 to 1/10 of the time of rise (T_r) of the hydrograph); (2) the speed of propagation (c') of a flow disturbance, i.e.,

$$c' = V + \sqrt{gD} \tag{2.6}$$

in which V is the flow velocity, g is the gravity acceleration constant, and D is the hydraulic depth of flow; and (3) the length of the reservoir (L_r). In order for the water surface to remain essentially level during each time step, the flow disturbance caused by the incoming flow at the upstream end of the reservoir must propagate through the entire length of the reservoir during the Δt time interval. When this does not occur, the water surface is not horizontal or level but rather has a sloping surface along the length of the reservoir.

In order to assess the magnitude of the error in the computed discharges via the level-pool routing algorithm when the water surface is not level, a number of reservoir routing applications having a range of reservoir properties (length, depth, volume) and a range of incoming discharge hydrographs were simulated with the level-pool reservoir routing algorithm as well as with a highly accurate implicit dynamic routing algorithm. The dynamic routing algorithm (Fread, 1974, 1977, 1978, 1985, 1988, 1992) is based on the complete one-dimensional (Saint-Venant) equations of unsteady flow; it accounts for sloping water surfaces as well as inertial effects ignored in the level-pool algorithm. The level-pool algorithm's outflow discharges were compared with those simulated by the dynamic routing algorithm. The difference between the two was considered to be the magnitude of the error associated with the level-pool algorithm when the reservoir routing application violated the basic assumption of a horizontal (level) water surface at all times during the routing.

The level-pool routing error (e_q), associated with the rising limb of the outflow hydrograph, is normalized by expressing it as a percent of the peak outflow discharge, i.e.,

$$e_q = 100 \left[\sum_{i=1}^{N'} \left(Q_{L_i} - Q_{D_i}\right)^2 / N' \right]^{1/2} \Big/ Q_{D_p} \tag{2.7}$$

in which Q_{L_i} is the level-pool routed flow; Q_{D_i} is the dynamic routed flow, Q_{D_p} is the dynamic routed flow peak, and N' is the number of computed discharges comprising the rising limb of the routed hydrograph.

The normalized level-pool routing error (e_q) is shown plotted in Fig. 1 as a function of three dimensionless parameters of time, length, and volume, i.e., σ_t, σ_ℓ, and σ_v respectively. They are defined as follows:

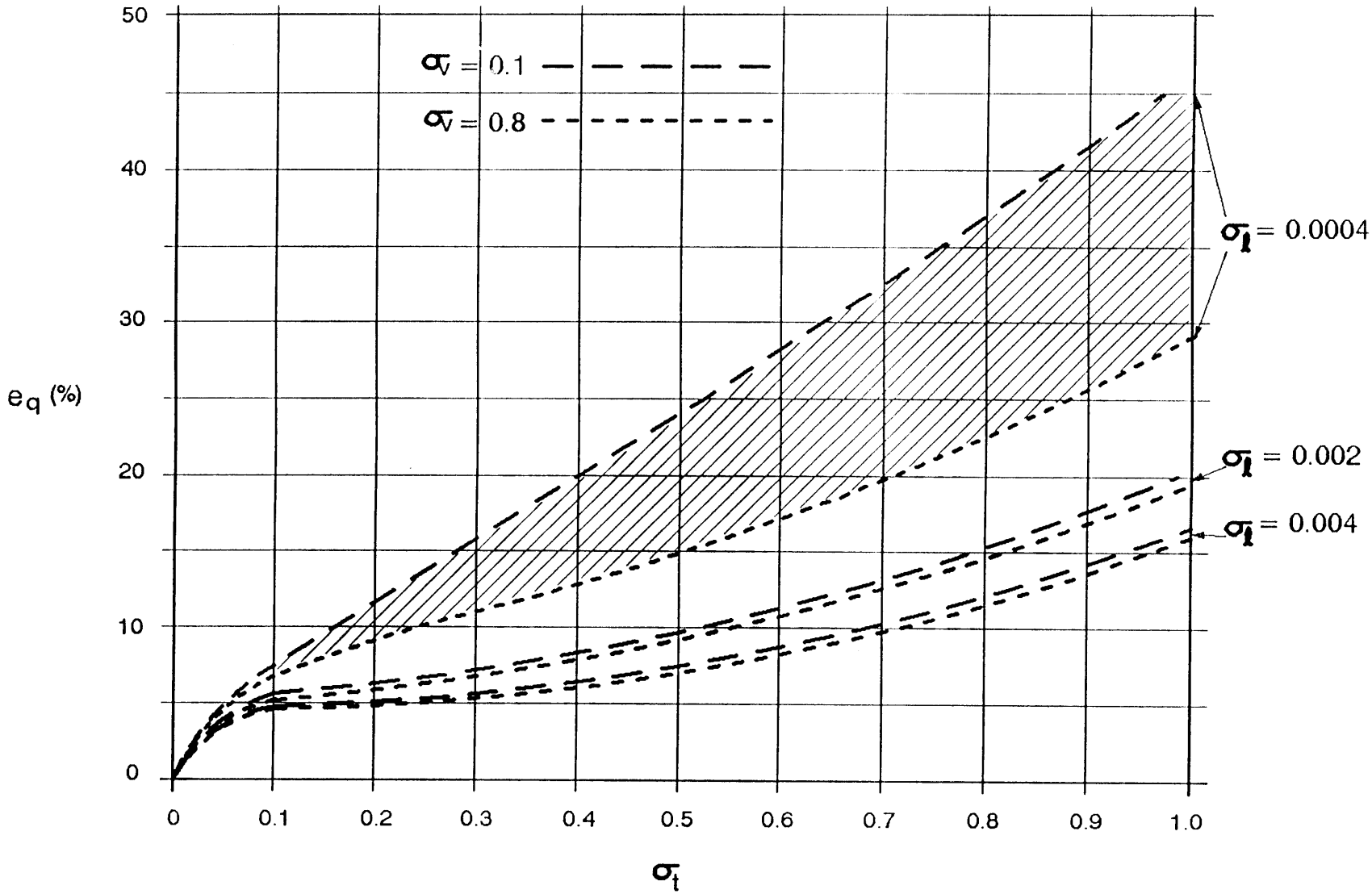

Fig. 1 Level-pool routing compared to dynamic routing showing the normalized error (E_q) of the rising limb of the outflow hydrograph as a function of σ_t, σ_l and σ_v (dimensionless parameters that reflect the reservoir volume, length, depth, and the inflow hydrograph volume and time of rise.)

$$\sigma_t = \mu\ L_r/(3600\ \ T_r\ \sqrt{gD_r}\ ) \tag{2.8}$$

$$\sigma_\ell = D_r/(\mu\ L_r) \tag{2.9}$$

$$\sigma_v = \text{hydrograph volume/reservoir volume} \tag{2.10}$$

in which μ is a units conversion factor having a value of 5280 (US) or 1000 (SI), g is the gravity acceleration constant, L_r is the reservoir length in miles (US) or km (SI), D_r is the average depth of the reservoir in ft (US) or m (SI), and T_r is time of rise of the hydrograph in hours.

An inspection of Fig. 1 reveals the following:

(1) e_q increases as σ_t increases; therefore, from Eq. (2.8), e_q increases as L_r increases, as T_r decreases, and as D_r decreases;

(2) e_q increases as σ_ℓ decreases; therefore, from Eq. (2.9), e_q increases as L_r increases, and as D_r decreases; and

(3) e_q increases as σ_v decreases; therefore, from Eq. (2.10), e_q increases as the hydrograph volume decreases and as the reservoir volume increases.

Fig. 1 can be used to obtain an estimate of the error incurred in level-pool routing if L_r = 150 miles, D_r = 300 ft, T_r = 6 hrs, and σ_v = 0.1. Using Eqs. (2.8) and (2.9), σ_t and σ_ℓ are computed as follows:

$$\sigma_t = \frac{\mu\ L_r}{3600\ \ T_r\ \sqrt{g\ D_r}} = \frac{5280\ \ 150}{3600\ \ 6\ \sqrt{32.2\ (300)}} = 0.37$$

$$\sigma_\ell = \frac{D_r}{\mu\ L_r} = \frac{300}{5280\ (150)} = 0.0004$$

Then, with σ_t = 0.37, σ_ℓ = 0.0004, and σ_v = 0.1, Fig. 1 can be interpolated to give a value of 18 percent for the routing error (e_q). However, if for the same reservoir, the hydrograph has much different properties such as T_r = 48 hrs and σ_v = 0.8, then recomputing σ_t, i.e.,

$$\sigma_t = \frac{\mu\ L_r}{3600\ \ T_r\ \sqrt{g\ D_r}} = \frac{5280\ \ 150}{3600\ \ 48\ \sqrt{32.2\ (300)}} = 0.05$$

and entering Fig. 1 with σ_t = 0.05, σ_ℓ = 0.0004, and σ_v = 0.8, a value of 5 percent for e_q is obtained. This illustrates the sensitivity of e_q to the properties of the hydrograph.

From Fig. 1, if the routing error (e_q) is restricted to less than 10 percent, then $\sigma_t \leq 0.2$, and $\sigma_t \geq 0.0004$. Using these values in Eqs. (2.8) and (2.9), the following semi-empirical equation can be derived for the minimum allowable time of rise ($T_{r\,min}$) necessary to restrict level-pool routing errors $e_q < 10$ percent:

$$T_{r\,min} = a/b \cdot L_r/\sqrt{D_r} \tag{2.11}$$

where:

$$b = \alpha/\sigma_t^{\beta} \tag{2.12}$$

and a = 0.26 (US) or 0.09 (SI); L_r has units of ft (US) or km (SI); D_r has units of ft (US) or m (SI); and $\alpha = 0.28$, $\beta = 0.21$ if $\sigma_t \leq 0.0004$ or $\alpha = 0.088$, $\beta = 0.66$ if $\sigma_t > 0.0004$.

If Eq. (2.11) is applied to a range of values for L_r and D_r, the minimum allowable values for T_r, which restrict e_q errors to less than 10 percent, are given in Table 1.

Table 1. Minimum Allowable T_r Values Computed from Eq. (2.11) for a Range of L_r and D_r Values such that $e_q < 10\%$

L_r (mi)	D_r (ft)	$T_{r\,min}$ (hr)		L_r (mi)	D_r (ft)	$T_{r\,min}$ (hr)
5	10	2.3		50	100	7.2
5	20	1.0		50	200	3.3
5	50	0.4		50	300	1.9
10	20	3.2		100	100	16.2
10	40	1.5		100	200	10.1
10	100	0.5		100	300	7.1
25	50	5.1		200	100	34.4
25	100	2.3		200	200	22.9
25	250	0.8		200	300	17.5

An inspection of Table 1 shows that, in general, level-pool routing errors exceeding 10 percent are associated with most reservoirs subjected to very rapidly rising hydrographs such

as dam-break floods or turbine releases, i.e., $0.1 < T_r < 1.0$. Also, for very long reservoirs ($L_r \geq 50$) flash floods or small tributary floods with $6 \leq T_r \leq 18$ will be subject to level-pool routing errors exceeding 10 percent. Finally, as D_r becomes increasingly smaller and L_r larger, level-pool routing for such "run-of-the-river" reservoirs is not applicable because the $T_{r_{min}}$ values exceed those of the routed hydrographs.

3.0 Muskingum-Cunge Diffusion Routing Algorithm and Error Properties

The well-known and much used Muskingum routing method was modified by Cunge (1969) so as to significantly increase its range of application from that of a kinematic wave-based routing method to one based on the diffusion analogy. This modified Muskingum method, known as the Muskingum-Cunge method, is most effectively used as a distributed flow routing technique.

3.1 Muskingum-Cunge Diffusion Routing Algorithm.

The Muskingum-Cunge recursive equation applicable to each Δx_i subreach for each Δt^j time step is:

$$Q_{i+1}^{j+1} = C_1 Q_i^{j+1} + C_2 Q_i^j + C_3 Q_{i+1}^j + C_4 \tag{3.1}$$

where:

$$C_1 = (\Delta t^j - 2KX)/C_5 \tag{3.2}$$

$$C_2 = (\Delta t^j + 2KX)/C_5 \tag{3.3}$$

$$C_3 = [2K(1-X) - \Delta t^j]/C_5 \tag{3.4}$$

$$C_4 = \bar{q}_i \, \Delta x_i \, \Delta t^j / C_5 \tag{3.5}$$

in which:

$$C_5 = 2K(1-X) + \Delta t^j \tag{3.6}$$

$$K = \Delta x_i / \bar{c} \tag{3.7}$$

$$X = 0.5[1 - \bar{Q}/(\bar{c}\,\bar{B}\,S_e\,\Delta x)] \tag{3.8}$$

The coefficients C_1, C_2, and C_3 are positive values whose sum must equal unity. The C_4 coefficient accounts for the effect of lateral flow ($\bar{q}_i$). K is a storage constant having the dimension of time, and X is a weighting factor expressing the relative importance of inflow and outflow on the storage in the Δx_i subreach. The bar (-) above the variable indicates the variable is averaged over the Δx_i subreach and over the Δt^j time step. In Eqs. (3.1) - (3.8), Q is discharge, S_e is the energy slope, $\bar{B}$ is the cross-sectional wetted topwidth, $\bar{c}$ is the kinematic wave celerity, i.e.,

$$\bar{c} = (5/3 - 2/3\ \bar{A}/\bar{B}^2\ d\bar{B}/dy)\ \bar{Q}/\bar{A} \tag{3.9}$$

in which dB/dy is the rate of change of the topwidth (B) with respect to the flow depth (y), and A is the cross-sectional wetted area.

It can be shown that Eq. (3.1) is a finite-difference approximation of the classical kinematic wave equation, i.e.,

$$\partial Q/\partial t + c\ \partial Q/\partial x - cq = 0 \tag{3.10}$$

However, Cunge (1969) demonstrated that if X is expressed as a particular function of the flow properties, i.e., Eq. (3.8), and if the storage constant (K) is expressed as in Eq. (3.7), then Eq. (3.1) is a finite-difference representation of the following parabolic diffusion analogy equation:

$$\partial Q/\partial t + c\ \partial Q/\partial x - cq - D_f\ \partial^2 Q/\partial x^2 = 0 \tag{3.11}$$

in which $D_f = (1-F^2/4)Q/(2\ B\ S_o)$ is a diffusion coefficient and $F = Q/\left(\sqrt{g/B}\ A^{3/2}\right)$ is the Froude number. Eq. (3.11) can account for wave attenuation. The kinematic wave Eq. (3.10) does not allow for the physical phenomenon of wave attenuation except through numerical errors introduced by the Δx and Δt computational steps.

For minimal numerical errors introduced in solving Eq. (3.1), the time step (Δt^j) and distance step (Δx_i) should be selected according to Jones (1981) as follows:

$$\Delta t \leq T_r/M \tag{3.12}$$

where $M \geq 5$, T_r is the time of rise of the hydrograph, and

$$\Delta x \simeq 0.5\ c\ \Delta t\left[1 + \left(1 + 1.5\ Q/(B\ c^2\ S_o\ \Delta t)\right)^{1/2}\right] \tag{3.13}$$

in which S_o is the channel bottom slope.

Solution technique. With coefficients defined by Eqs. (3.2) - (3.8), Δt and Δx selected according to Eqs. (3.12) and (3.13) respectively, the Muskingum-Cunge recursive diffusion routing equation can be solved by either linear or nonlinear (iterative) methods.

In the linear method, the space and time averaged variables ($\bar{Q}$, $\bar{B}$, $\bar{A}$) are computed from the known values (Q_i^j, Q_{i+1}^j, Q_i^{j+1}) within the Δx_i subreach, i.e.,

$$\bar{Q} = (Q_i^j + Q_{i+1}^j + Q_i^{j+1})/3 \tag{3.14}$$

Eq. (3.14) is not a very good average since it neglects the unknown value of (Q_{i+1}^{j+1}). This causes unwanted and significant errors in the solution of Eq. (3.1).

In the nonlinear method, the space and time averaged variables ($\bar{Q}$, $\bar{B}$, $\bar{A}$) include the unknown value Q_{i+1}^{j+1} which requires an iterative procedure since Q_{i+1}^{j+1} must be first estimated as $\hat{Q}_{i+1}^{j+1}$ from a previous time or iteration step, i.e.,

$$\bar{Q} = (Q_i^j + Q_{i+1}^j + Q_i^{j+1} + \hat{Q}_{i+1}^{j+1})/4 \tag{3.15}$$

Iteration ceases when $|Q_{i+1}^{j+1} - \hat{Q}_{i+1}^{j+1}| < \epsilon$, where ϵ is a small acceptable tolerance value.

Computation of water-surface elevations. The water-surface elevation (h) corresponding to each discharge must also be computed since B and A in Eqs. (3.8) and (3.9) are known functions of h; also, the determination of the water-surface elevation is usually an important result, in addition to discharge, that is desired from the flood routing computations. The water-surface elevations may be obtained using a steady, uniform flow formula such as the Manning equation, i.e.,

$$Q = \mu'/n \; AR^{2/3} \; S_e^{1/2} \tag{3.16}$$

in which n is the Manning roughness coefficient, A is the cross-sectional area, R is the hydraulic radius given by A/P in which P is the wetted perimeter of the cross section, S_e is the energy slope computed via a backwater equation for only the initial flow to properly approximate S_e for channels with irregular and even adverse bottom slopes, and μ' is a units conversion factor (1.49 for US and 1.0 for SI). Eq. (3.16) is solved for the depth by iterative numerical techniques such as Newton-Raphson method and, if nonconvergence occurs, followed by the less efficient bi-section method.

3.2 Error Properties of Muskingum-Cunge Routing

In order to assess the magnitude of errors associated with the nonlinear Muskingum-Cunge routing algorithm with water-surface elevations computed from the normal depth Manning Eq. (3.16), a number of routing applications having a range of hydrographs and channel

bottom slopes were simulated with the Muskingum-Cunge method as well as with a highly accurate implicit dynamic routing algorithm (Fread, 1988, 1992). The Muskingum-Cunge algorithm's peak discharges and corresponding water-surface elevations were compared with those computed by the dynamic routing algorithm. The difference between the two was considered to be the magnitude of the error associated with the Muskingum-Cunge algorithm. The Muskingum-Cunge peak routing error ($\bar{\epsilon}$) expressed in percent is:

$$\bar{\epsilon} = (\epsilon_Q^2 + \epsilon_h^2)^{1/2} \tag{3.17}$$

where:

$$\epsilon_Q = 100(Q_{M_p} - Q_{D_p})/Q_{D_p} \tag{3.18}$$

$$\epsilon_h = 100\,(h_{M_p} - h_{D_p})/h_{D_p} \tag{3.19}$$

in which Q_{M_p} and h_{M_p} are the peak discharge and water-surface elevation computed by the Muskingum-Cunge algorithm, while Q_{D_p} and h_{D_p} are the peak discharge and water-surface elevations computed by the dynamic routing algorithm.

Previously, Fread (1983, 1985) derived the following theoretical error expression for general diffusion routing algorithms:

$$T_{r_{min}} = \mu''\ \phi'\ q_p^{0.4}/(\bar{\epsilon}\ n^{0.6}\ S^{0.7}) \tag{3.20}$$

in which μ'' is a units conversion factor, 0.0022 (US) or 0.0091 (SI), ϕ' is a channel shape factor (0.55 for natural channels with flood plains, 0.6 for rectangular-, 0.54 for parabolic-, and 0.50 for triangular-shaped channels), q_p is the peak discharge per unit width of channel, S is the channel bottom slope, ft/ft, and $T_{r_{min}}$ is the minimum time of rise of the routed hydrograph compatible with the routing error, $\bar{\epsilon}$. A sensitivity analysis of Eq. (3.20) indicates the terms (ϕ', $q_p^{0.4}$, $n^{0.6}$) have maximum influence on $T_{r_{min}}$ by factors representing the ratio of the maximum/minimum values of each term, i.e., 1.2, 2.0, 2.5, respectively; however, $S^{0.7}$ has an influence ratio of at least 40. Therefore, the only parameter that can greatly affect the minimum allowable time of rise ($T_{r_{min}}$) for an allowable error ($\bar{\epsilon}$) is S. Thus the following expression can be used to approximate Eq. (3.20):

$$T_{r_{min}} = u/S^{v} \tag{3.21}$$

in which u and v are fitting parameters.

The results of this empirical error analysis via comparative routings through 10-, 20-, 50-, and 100-mile channel reachs are shown in Fig. 2. The curves representing a constant value of $\bar{\epsilon}$ are plotted against the dominant hydrograph property, T_r (the time of rise in hrs)

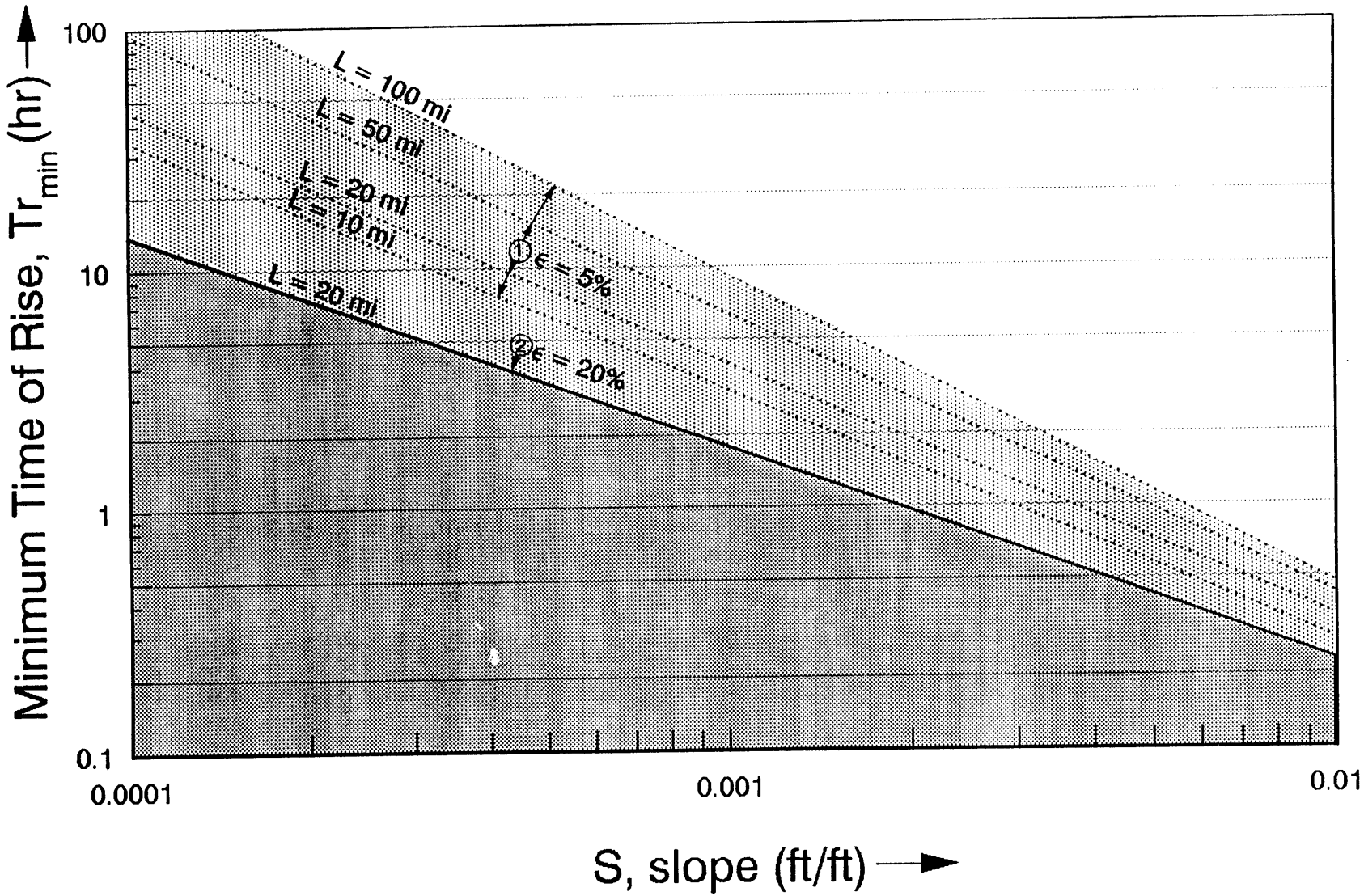

Fig. 2 Error (ϵ) levels of Muskingum-Cunge Diffusion Routing Algorithm shown in relation to the minimum allowable time of rise (Tr) and bottom slope (S).

along the vertical axis, and S_o (the average channel bottom slope, in ft/ft) along the horizontal axis. The Muskingum-Cunge algorithm is shown for 5 percent and 20 percent $\bar{\epsilon}$ curves, i.e., curve #1 (for routing reaches of 10, 20, 50, and 100 miles) and curve #2 (for the 20-mile routing reach only), respectively. In general these curves show that as S increases, there is a gradual nonlinear decrease in the minimum T_r values that can be accommodated by the algorithm for a given $\bar{\epsilon}$ value. The 5 percent curves are located above the 20 percent curve; this denotes that the minimum T_r values increase as the error $\bar{\epsilon}$ decreases. In general, Fig. 2 indicates that the Muskingum-Cunge algorithm is not applicable for rapidly rising hydrographs such as dam-break floods or turbine releases (say $T_r < 4$) for flat channels (say $S < 0.001$ ft/ft or approximately 5 ft/mile). The minimum allowable T_r gradually decreases to about 0.3 hr as the slope increases to 0.01 (53 ft/mi). The darker shaded area represents all conditions of S and T_r that cause the error $\bar{\epsilon}$ to exceed 20 percent while the unshaded area represents all S and T_r values that produce $\bar{\epsilon}$ values less than 5 percent. The lighter shaded area represents the conditions of S and T_r that cause the routing error to be within the range $5\% \leq \bar{\epsilon} \leq 20\%$. The 5 percent $\bar{\epsilon}$ curve #1 for the routing reach (L = 20 mi) can be represented by an expression similar in form to Eq. (3.21) for the minimum allowable T_r, i.e.,

$$T_{r_{min}} = 0.0026/S^{1.06} \tag{3.22}$$

Also, the 20 percent $\bar{\epsilon}$ curve #2 for the routing reach (L = 20 mi) can be expressed in a similar manner, i.e.,

$$T_{r_{min}} = 0.0031/S^{0.92} \tag{3.23}$$

The routing reach length (L) affects the routing error as shown by the four dashed curves for $\epsilon = 5\%$ for reach lengths of 10, 20, 50, and 100 miles. The error increases with L but in a nonlinear manner in which the increase dampens as the slope(S) increases.

In general, those routing applications involving a gently sloping channel and rapidly rising floodwave such as dam-break floods or turbine releases, when the combination of S_o and T_r becomes small enough that Eq. (3.22) cannot be satisfied, dynamic routing models are required. Also, dynamic routing models are required for (a) situations where backwater effects are important due to tides, significant tributary inflows, natural constrictions, dams, and/or bridges; and (b) situations where waves propagate upstream from large tides and storm surges or very large tributary inflows. As the trend for increased computer computa-tional speed and storage capabilities at decreased costs continues, the economic feasibility of using dynamic routing models for a wider range of applications will continue to increase, since dynamic models have the capability to correctly simulate the widest spectrum of wave types and waterway characteristics. Implicit dynamic routing models -- the most efficient and versatile although the most complex of the dynamic routing models -- will be increasingly utilized as improvements continue to be made in their computational robustness and reliability. Actually, the required computer time for the NWS implicit dynamic routing model (DAMBRK) is only about twice that required for the Muskingum-Cunge routing algorithm.

4.0 Selection of Δx and Δt Parameters for Implicit Dynamic Routing Models

Four-point implicit finite-difference approximation equations of the complete Saint-Venant unsteady flow equations constitute the most extensively used basis of implicit dynamic routing models such as the NWS DAMBRK (Dam-Break), DWOPER (Dynamic Wave Operational) and FLDWAV (Flood Wave) river/reservoir routing models (Fread, 1974, 1977, 1978, 1985, 1988, 1992; Fread and Lewis, 1988). It is most important that appropriate computational distance (Δx) and time step (Δt) parameters be used in the application of these routing models. If the selected values are too small, the computations are inefficient, sometimes to the extent of making the application too expensive or time consuming and therefore infeasible; however, if the values are too large, the resulting truncation error (the difference between the true solution of the partial differential Saint-Venant equations and the approximate solution of the four-point implicit finite-difference approximations of the Saint-Venant equations) may be so large that the computed solution of discharge and corresponding water-surface elevation is totally unrealistic. Unrealistic solutions can cause the computer program to abort when computed elevations result in negative depths; also, unrealistic solutions can result in significant irregularities in the computed hydrograph as manifested by spurious spikes in the rising and/or falling limbs of the hydrograph.

After several years of experience with the selection of Δx and Δt values for the NWS implicit dynamic routing models in numerous applications, the following empirical selection formulae were developed:

$$\Delta t \simeq T_r/20 \tag{4.1}$$

and,

$$\Delta x \leq c\, T_r/20 \tag{4.2}$$

where T_r is the hydrograph's time of rise (time from the significant beginning of increased discharge to the peak of the discharge hydrograph), in hours; and c is the bulk wave speed (the celerity associated with an essential characteristic of the unsteady flow such as the peak or center of gravity of the hydrograph), in miles/hour; Δt is the computational time step size, in hours; and Δx is the computational distance step size, in miles. In most applications, the bulk wave speed is well approximated as a kinematic wave celerity; it can also be approximated from two or more observed flow hydrographs at different points along the waterway. Since c can vary along the waterway (channel, river, reservoir, estuary), Δx may not be constant along the waterway. The kinematic wave celerity can be approximated for rivers as follows:

$$c \simeq k' V \tag{4.3}$$

in which k' is the kinematic wave ratio having values ranging from $4/3 \leq k' \leq 5/3$ ($k' \simeq 3/2$ for most natural channels), and V is the flow velocity.

Recently, a theoretical derivation of selection criteria for Δx and Δt computational parameters was achieved. The new criteria not only explain the utility of the previous empirical formulae in generally producing acceptable computational results, but are also capable of yielding appropriate Δx and Δt values for routing applications significantly differing from past experience. A derivation of the new Δx and Δt selection criteria follows.

Theoretical wave damping (attenuation) and celerity (velocity) error diagrams were obtained previously by Fread (1974) using a Fourier technique similar to that used by Leendertse (1967) on the linearized Saint-Venant equations. The error diagrams consisted of convergence ratios (the ratio of the implicit finite-difference solution of the linearized equations to their analytical solution) for wave damping and celerity which were plotted against D_L (the wave discretization number) for a range of D_C (Courant number) values and dimensionless friction (D_f) values. Recently, it was observed that a relationship between D_L and D_C could be established for error (e) values in the range of 0 to 5 percent. This relationship was of the form:

$$D_L \geq \eta \, D_C \tag{4.4}$$

where η is approximately 12 for $e \simeq 2$ percent, and $\eta \simeq 7$ for $e \simeq 5$ percent.

The wave discretization number (D_L) is defined as:

$$D_L = L_w/\Delta x \tag{4.5}$$

where L_w is the wave length and Δx is the computational distance step. However,

$$L_w = c\,T \simeq c\,3\,T_r \tag{4.6}$$

where c is the kinematic wave celerity, T is the wave period of the unsteady disturbance (wave), and T_r is the time of rise of the wave or hydrograph. Substituting Eq. (4.6) into Eq. (4.5) yields:

$$D_L = 3\,c\,T_r/\Delta x \tag{4.7}$$

The Courant number (D_C) is defined as:

$$D_C = c'\,\Delta t/\Delta x \tag{4.8}$$

where the dynamic wave celerity (c') is:

$$c' = V + \sqrt{gD} \tag{4.9}$$

in which V is flow velocity, g is the gravity acceleration constant, and D is the hydraulic depth of flow.

4.1 Δx Selection Criteria

Substituting Eq. (4.7) into Eq. (4.4) yields:

$$3\ c\ T_r\ /\ \Delta x \geq \eta\ D_C \tag{4.10}$$

which can be rearranged to give:

$$\Delta x \leq \frac{c\ T_r}{\eta\ D_C/3} \tag{4.11}$$

If η is replaced with the conservative value of 12, i.e., a 2 percent level of truncation error is tolerated, and if $D_C \geq 5$, then

$$\Delta x \leq c\ T_r/20 \tag{4.12}$$

which is identical with the empirical formula for Δx selection, i.e, Eq. (4.2).

The Δx selection criterion, Eq. (4.12), is based on the linearized form of the Saint-Venant equations; however, the complete Saint-Venant equations used in the NWS implicit routing models are nonlinear. The nonlinear terms can interact with highly nonlinear data (severe expansion/contraction in cross-sectional area or significant changes in bottom slope along the waterway) so as to require even smaller Δx computational distance steps than specified by Eq. (4.12).

Thus, another criterion for the selection of Δx is the restriction imposed by rapidly varying cross-sectional changes along the waterway. Samuels (1985) found that, for severely contracting/expanding cross sections, the four-point implicit finite-difference solution theoretically requires the following criterion be satisfied within any Δx computational distance step:

$$0.635 < A_{i+1}\ /\ A_i < 1.576 \tag{4.13}$$

in which A_i and A_{i+1} are the wetted cross-sectional areas at adjacent locations, i and i+1, along the waterway. Basco (1987) found from numerical experimental studies using NWS DAMBRK the following similar criterion:

$$0.70 < A_{i+1}/A_i < 2.0 \tag{4.14}$$

Fread (1988) developed the following algorithm to ensure that the selected computational distance step satisfied the criterion of Eq. (4.13):

$$\Delta x = \Delta X_i / N'' \tag{4.15}$$

where:

$$N'' = 1 + 2\ |A_i - A_{i+1}|/\hat{A} \tag{4.16}$$

in which ΔX_i is the preliminary distance step, $\hat{A}=A_{i+1}$ if $A_i > A_{i+1}$ (contracting reach) or $\hat{A}=A_i$ if $A_i < A_{i+1}$ (expanding reach), and N'' is rounded to the nearest smaller integer value.

Also, significant changes in the bottom slope of the waterway can require small computational distance steps in the vicinity of the change. This is required particularly when the flow changes from subcritical flow ($V/\sqrt{gD} < 1$) to supercritical flow ($V/\sqrt{gD} > 1$) or conversely along the waterway. Such changes can require Δx computational distance steps as small as:

$$\Delta x_{mn} < \Delta x < \Delta x_{mx} \tag{4.17}$$

in which Δx_{mn} = 0.01 miles (16m) and Δx_{mx} = 0.038 miles (61m).

The appropriate Δx selection would be that given by Eq. (4.12) unless in Eq. (4.16) when $N'' > 1$, a smaller Δx would result from Eq. (4.15), or if Eq. (4.17) were applicable which could require smaller Δx than either Eq. (4.12) or Eq. (4.15).

4.2 Δt Selection Criterion

In order to find an expression for the selection of Δt, Eq. (4.7) and Eq. (4.8) are substituted into Eq. (4.4). This gives:

$$3\ c\ T_r / \Delta x \geq \eta\ c'\ \Delta t/\Delta x \tag{4.18}$$

which can be rearranged to give:

$$\Delta t \leq T_r/M \tag{4.19}$$

where:

$$M = \eta\ c'/(3\ c) \tag{4.20}$$

Replacing η with the conservative value of 12 which allows a 2 percent level of truncation error, and substituting Eq. (4.3) and Eq. (4.9) into Eq. (4.20) yields:

$$M = 4\ (V + \sqrt{gD})/(1.5V) \tag{4.21}$$

Now, the Manning equation is used for V, i.e.,

$$V = \mu' \, D^{2/3} \, S_o^{1/2}/n \tag{4.22}$$

in which μ' is 1.49 (US units) and 1.0 (SI units), D is the hydraulic depth of flow in the river, S_o is the bottom slope (dimensionless), and n is the Manning roughness coefficient. And substituting Eq. (4.22) into Eq. (4.21) gives:

$$M = 2.67\left[1 + \tilde{\mu} n/(D^{1/6} \, S_o^{1/2})\right] \tag{4.23}$$

in which $\tilde{\mu}$ is 3.78 (US units) and 3.13 (SI units). Using typical values for S_o, n, and D as shown in Table 2, Eq. (4.23) provides a range of M values of $8 \leq M \leq 33$. For other

Table 2. M values computed from Eq. (4.23) for a range of S_o, n, and D values

S_o (ft/mile)	S_o (ft/ft)	n	D (ft)	M
100	0.01894	0.070	5	7
25	0.00473	0.040	10	7
5	0.00095	0.035	20	10
1	0.00019	0.030	20	16
0.5	0.000095	0.015	30	12
0.5	0.000095	0.035	10	28

practical values of S_o, n, and D, the range for M could be somewhat greater but generally not exceeding $6 \leq M \leq 30$. Thus, Eq. (4.19) with an M value of 20 is the same as Eq. (4.1). Eqs. (4.19) and (4.23) indicate that Δt should be more variable than allowed in Eq. (4.1) due to the influence of the channel hydraulic properties (S_o, n, and D), with the latter property a function of the channel cross-sectional shape and size. Also, it is recommended that Eq. (4.23) be used for M in Eq. (3.12) to select Δt for the Muskingum-Cunge diffusion routing algorithm.

5.0 Recent Improvements in the NWS SMPDBK Model

The NWS Simplified Dam-Break (SMPDBK) Flood Forecasting Model was first developed in the early 1980's and released in 1984 (Wetmore and Fread, 1984). It was

considerably enhanced and released again in 1988. Recently, it was further improved and released in late 1991 (Fread, et al., 1991).

5.1 Peak Flow Computation

The SMPDBK model consists of a peak discharge (Q_p) equation which considers the time-dependent breach of a dam and the possible submergence effects (reduction in the peak outflow) due to the downstream water-surface elevation, i.e.,

$$Q_p = K_s \left[Q_o + 3.1\ B_r \left(C/(t_f/60 + C/\sqrt{H}\ ) \right)^3 \right] \tag{5.1}$$

where:

$$C = 23.4\ Sa/B_r \tag{5.2}$$

$$K_s = 1.0 \qquad \text{if } h_r \leq 0.67 \tag{5.3}$$

$$K_s = 1.0\text{-}27.8\ (h_r - 0.67)^3 \qquad \text{if } h_r > 0.67 \tag{5.4}$$

$$h_r = (h_t - h_b)/h_w \tag{5.5}$$

$$h_w = \left[C/(t_f/60 + C/\sqrt{H}\ ) \right]^2 \tag{5.6}$$

in which K_s is the submergence correction factor, Q_o (ft^3/sec) is the spillway and overtopping flow, B_r is the average breach width (ft), t_f is the duration of time (minutes) in which the breach linearly forms completely, Sa is the reservoir surface area (acres), h_t is the water-surface elevation (ft) in the tailwater section during peak flow, h_b is the final elevation (ft) of the breach bottom, and H is the reservoir water-surface elevation at initiation of breaching minus h_b.

The water-surface elevation (h_t) of the tailwater section just downstream of the dam is obtained from an iterative solution of the Manning Eq. (3.16), in which the energy slope (S_e) is computed as follows:

$$S_e = S_o + \Delta h_t/\Delta t \left[1/c + VB_t(1 - V/c)/gA_t \right] - 1/g\ \Delta V/\Delta t \tag{5.7}$$

in which $V = Q_p/A_t$ and c is the kinematic wave speed defined by Eq. (3.9).

The iterative solution utilizes the Newton-Raphson method which is very efficient; however, occasionally it does not converge. When convergence is not attained in 15 iterations, the more reliable but less efficient bi-section method is used. Since h and S are interdependent, h is always solved twice. First, Eq. (3.16) is solved for h_t using S_o for S_e. Then using this value for h_t in Eq. (5.7), S_e is computed and Eq. (3.16) is once again solved for h_t.

The use of Eq. (5.7), rather than assuming $S_e = S_o$, is among the improvements of the most recent release of SMPDBK. Another recent enhancement involves the procedure to obtain a first estimate for K_s. In some applications, the submergence correction factor that was obtained in previous versions was not correct, particularly if there was considerable submergence effects. The new enhancement always requires the associated tailwater (h_t) to be below the reservoir water-surface elevation. It is adjusted iteratively until the peak discharge does not change as the tailwater h_t is recomputed.

In three particular applications, the use of Eq. (5.7), along with the improved iteration scheme for K_s, reduced the error associated with the peak discharge (Q_p) by an average of 92 percent. The average residual error (as determined by comparing with the NWS DAMBRK model) was approximately 3 percent. In two of the applications, the former method computed K_s values of 0.79 and 0.46 when in fact they both should have been 1.0; these were obtained using the recent enhancements. In the other application, the old K_s value of 0.26 was found by the new method to be 0.79. In each of these applications, a larger and more accurate peak discharge was predicted by the recent enhancements to the SMPDBK model.

5.2 Peak Flow Routing and Water-Surface Elevation Computation

In the SMPDBK model, the peak discharge computed from Eq. (5.1) is routed (the peak is attenuated) to other points of interest downstream of the dam using dimensionless peak flow routing curves. These curves were developed from numerous executions of the implicit dynamic routing model, NWS DAMBRK (Fread, 1977, 1988, 1992). The curves are grouped as three families associated with specific peak flow Froude (F) numbers (0.25, 0.50, 0.75). The curves within a family are denoted by five dimensionless volume parameter (reservoir volume/wetted volume of downstream valley from dam to point of interest) values. Each curve shows the relationship of the dimensionless discharge ratio (routed peak/Q_p) to the dimensionless distance ratio (distance from dam to point of interest/X_c) in which X_c is a characteristic distance which is a function of the reservoir volume. The Manning Eq. (3.16), along with Eq. (5.7), is iteratively solved for the water-surface elevation (h) corresponding to the routed peak discharge.

5.3 Time of Travel Computation

The time of travel (TT_i) for the dam-break wave to propagate from the dam to the ith point of interest (x_i miles) downstream is computed as follows:

$$TT_i = t_f/60 + (\mu/3600)\, x_i/c_i \tag{5.8}$$

in which the wave speed (c_i) is computed the same as the kinematic wave speed defined by Eq. (3.9), and μ is a units conversion factor defined in Eq. (2.8) and Eq. (2.9).

In 1988, SMPDBK was improved to allow floodplains to have dead (off-channel) sections in addition to the active section. The total area (active + dead) was used to compute routed peak flows while the corresponding water-surface elevations were computed

using the Manning Eq. (3.16) with the cross-sectional area (A) consisting only of the active portion. It was noticed that in applications in which the downstream valley floodplain contained significant portions of dead (off-channel) storage, the flood wave celerity computed by Eq. (3.9) was too large although the routed peak discharge and corresponding water-surface elevations were in close agreement with those computed by the NWS DAMBRK model. In two particular applications, the averaged celerity error was 44 percent.

In the recent improvements to SMPDBK, the wave celerity used in Eq. (5.8) was computed as in Eq. (3.9); however the cross-sectional area (A) used in Eq. (3.9) is taken as the total cross-sectional area (active + dead). This resulted in a reduction in the celerity error of 63 percent in one application and 18 percent in another. The residual error in each were 39 percent and 15 percent, respectively.

6.0 Threshold Runoff for Areal Flash Flood Guidance

Part of the mission of the NWS River Forecast Centers (RFCs) is the preparation and distribution of flash flood guidance products. These products contain the rainfall amounts required to produce flooding,and are used by the Weather Forecast Offices (WFOs) as the criteria for issuing flash flood watches and warnings.

The principal flash flood guidance product is areal flash flood guidance. This is the average rain needed over an area during a specified time period (1-, 3-, 6-hour) to initiate flooding on small streams. Flooding is assumed to occur when the streamflow slightly exceeds bank-full capacity. Most of the small streams are ungaged. Currently, areal flash flood guidance is issued for zones, counties, and/or urban areas.

With the modernization of NWS during the 1990's, areal flash flood guidance will be issued on a gridded basis to be compatible with the fine resolution gridded precipitation estimates provided by the Weather Surveillance Radars (WSR-88D) installed throughout the United States under the Next Generation Weather Radar (NEXRAD) portion of the NWS modernization program. The modernized gridded areal flash flood guidance as described by Sweeney (1991) will be more accurate and consistent. Unlike the current areal guidance which is produced by hydrologic algorithms that vary considerably among the 13 RFCs, the modernized gridded areal flash flood guidance will be based on a uniform and objective methodology.

Two parameters are required to compute areal flash flood guidance. One is the threshold runoff value, i.e., the amount of runoff to cause slightly greater than bank-full flow in the small streams. The second is the current soil moisture conditions which affect the proportion of precipitation becoming runoff which enters the streams. Only the first component is addressed in detail in this paper.

6.1 Threshold Runoff Computation

The amount of runoff needed over an area to initiate flooding (streamflow slightly in excess of bank-full capacity) is the threshold runoff. Threshold runoff depends on several characteristics of the watershed and the stream channels. The size of the watershed (area) determines the total volume of water that appears downstream at a point of interest. The slope of the channel and roughness of the steambed controls the velocity of the water as it moves downstream. The following is a derivation for the threshold runoff algorithm as described by Sweeney (1991).

Snyder (1938) developed a method for determining excess runoff peak flow for ungaged basins. The method is based on the unit hydrograph principle, i.e., peak discharge (q_p) per unit of drainage area in acres (A_w) is a simple inverse function of the basin lag (t_p). Thus,

$$q_p = 640\ C_p/t_p \tag{6.1}$$

where q_p is in ft^3/sec/acres, t_p is in hours, and C_p is a parameter (ranging from about 0.4 to 0.8) obtained from a similar watershed that is gaged.

The basin lag was found by Snyder to be a function of basin size, shape, and slope, i.e.,

$$t_p = C_t\ (LL_c/\sqrt{S})^b \tag{6.2}$$

where t_p is the basin lag in hours, defined as the time from the centroid of rainfall to the peak of the unit hydrograph; C_t is the coefficient to be derived from similar watersheds that are gaged in the same region (generally varies from 0.35 for valley areas, 0.72 for foothill areas, to 1.2 to mountainous areas); L is the main stream length in miles from outlet to the upstream basin boundary; L_c is the main stream length in miles from the outlet or point of interest to a point on the stream nearest the watershed centroid; S is the weighted channel slope in feet per mile; and b is a constant assumed to be 0.38 (Linsley, et al., 1986).

If q_{pR} is the unit hydrograph peak discharge per unit area corresponding to unit volume of runoff (excess rainfall) of duration t_R, the peak discharge (Q_p) at the watershed outlet or point of interest corresponding to a volume R of runoff of duration t_R is:

$$Q_p = q_{pR}RA_w \tag{6.3}$$

where A_w is the area in square miles of the watershed upstream of the outlet or the point of interest; R is the runoff amount in inches; and Q_p is the peak discharge in ft^3/sec at the point of interest.

Q_p at bank-full flow can be related to channel geometrical and roughness characteristics using the Manning Eq. (3.16). It is convenient to consider the effect of channel shape by

representing the channel topwidth (B) as a power function of depth (y) with y_b denoting the bank-full depth and B_b the bank-full width, i.e.,

$$B_b = k\ y_b^m \tag{6.4}$$

in which k is a scale factor and m is a shape factor (0.25 for natural channels with floodplains, and 0 for rectangular-, 0.5 for parabolic-, and 1 for triangular-shaped channels). Integration of Eq. (6.4) with respect to depth provides an expression for the channel bank-full cross-sectional area, i.e.,

$$A_b = k\ y_b^{m+1}/(m+1) \tag{6.5}$$

Using Eq. (6.4) and Eq. (6.5), the term $AR^{2/3}$ ($R \simeq A/B$) in the Manning Eq. (3.16) can be expressed in the following form:

$$A_b R_b^{2/3} = B_b\ [y_b/(m+1)]^{5/3} \tag{6.6}$$

Thus the Manning Eq. (3.16) takes the following form for bank-full flow when using the local channel bottom slope (S_c) forthe energy slope (S_e):

$$Q_p = 1.486\ S_c^{1/2}/n\ \ B_b[y_b/(m+1)]^{5/3} \tag{6.7}$$

When the parameters to compute Q_p in Eq. (6.7) are not available from site observations, it has been found that an alternative to computing Q_p is to use, if available, a two-year return period flow (the flow expected to be equalled or exceeded once in two years).

Snyder used for the standard duration of rain (t_r), a value of $t_p/5.5$. For any other rain duration (t_R), the adjusted basin lag (t_{PR}) is given by the following:

$$t_{PR} = t_p + (t_R - t_p/5.5)/4 \tag{6.8}$$

which reduces to the following:

$$t_{PR} = 0.955\ t_p + 0.25\ t_R \tag{6.9}$$

Substitution of Eq. (6.2) into Eq. (6.9) yields the following expression for the adjusted basin lag (t_{PR}):

$$t_{PR} = 0.955\ C_t\ (LL_c/\sqrt{S})^{0.38} + 0.25\ t_R \tag{6.10}$$

Upon performing the following steps:

(1) substitute Eq. (6.10) into Eq. (6.1) for t_p and then substitute the resulting expression for q_p into Eq. (6.3) for q_{PR},

(2) substitute Eq. (6.7) into Eq. (6.3) for Q_p, and

(3) rearrange the expanded Eq. (6.3) to solve for R;

the following expression for threshold runoff is obtained:

$$R = \frac{0.00232\ B_b S_c^{0.5}}{n\ A_w\ C_p} \left[\frac{y_b}{m+1}\right]^{5/3} \left[0.955\, C_t \left[\frac{L L_c}{S^{0.5}}\right]^{0.38} + 0.25\, t_r\right] \tag{6.11}$$

where R is the threshold runoff in inches which will cause bank-full flow at the point of interest; B_b is the bank-full width in feet; S_c is the local stream bottom slope in feet per feet; y_b is the bank-full depth in feet; C_t is a coefficient described in Eq. (6.2); L is the length of stream in miles from point of interest to upstream end; L_c is the length of the stream in miles from the point of interest to the centroid of the area; S is the weighted channel slope throughout the drainage area in feet per mile; t_r is the duration of rainfall in hours; A_w is the drainage area in square miles upstream of the point of interest; C_p is a coefficient described in Eq. (6.1); m is the channel shape parameter defined in Eq. (6.4); and n is the Manning roughness coefficient which can be estimated for in-bank flows by an expression developed by Barrett (1984), i.e.,

$$n = \psi\ S_c^{0.38}/(A_b/B_b)^{0.16} \tag{6.12}$$

in which ψ = 0.39 (US) or 0.32 (SI), A_b is the bank-full cross-sectional area, and n must be $\geq$ 0.03.

The watershed geometric parameters (L, L_c, S, and A) can be obtained automatically via Geographical Information Software (GIS) packages, digital terrain elevation databases, and specific software algorithms. Such a combined software package called Gridded Threshold Runoff (GTR) has been developed for NWS by the University of Iowa using the GIS software package, GRASS.

The channel parameters (B_b, y_b, and m) can be obtained by representative site inspections. These parameters are then regressed against upstream watershed area (A_w) and weighted slope (S) to obtain the channel parameters at all desired points of interest. The local channel slope (S_c) is also obtained from the GTR software package. The Manning n is estimated from Eq. (6.12).

Of the remaining parameters (C_p, C_t, and t_r) in Eq. (6.11), t_r is selected as either 1 hr, 3 hr, or 6 hr, and C_p and C_t are calibrated from similar gaged watersheds for which unit hydrographs are available.

6.2 Gridded Threshold Runoff Values

The GTR determines the geographic locations of the network of streams that drain all sub-basins having a specified minimum-sized watershed. The GTR then computes the threshold runoff (R) values for sub-basins as indicated by the dashed lines in Fig. 3. Starting upstream, GTR locates all stream junctions using a sub-basin area of at least 6.25 mi^2. Next the total area is computed upstream of each subjunction. This process establishes a stream network grid which is nonuniform. An interpolation algorithm is used to provide the threshold runoff values for a uniform grid network as shown in Fig. 3. The uniform grid network -- a multiple of the 4 km x 4 km grid of the WSR-88D precipitation estimates -- is superimposed over the stream network grid.

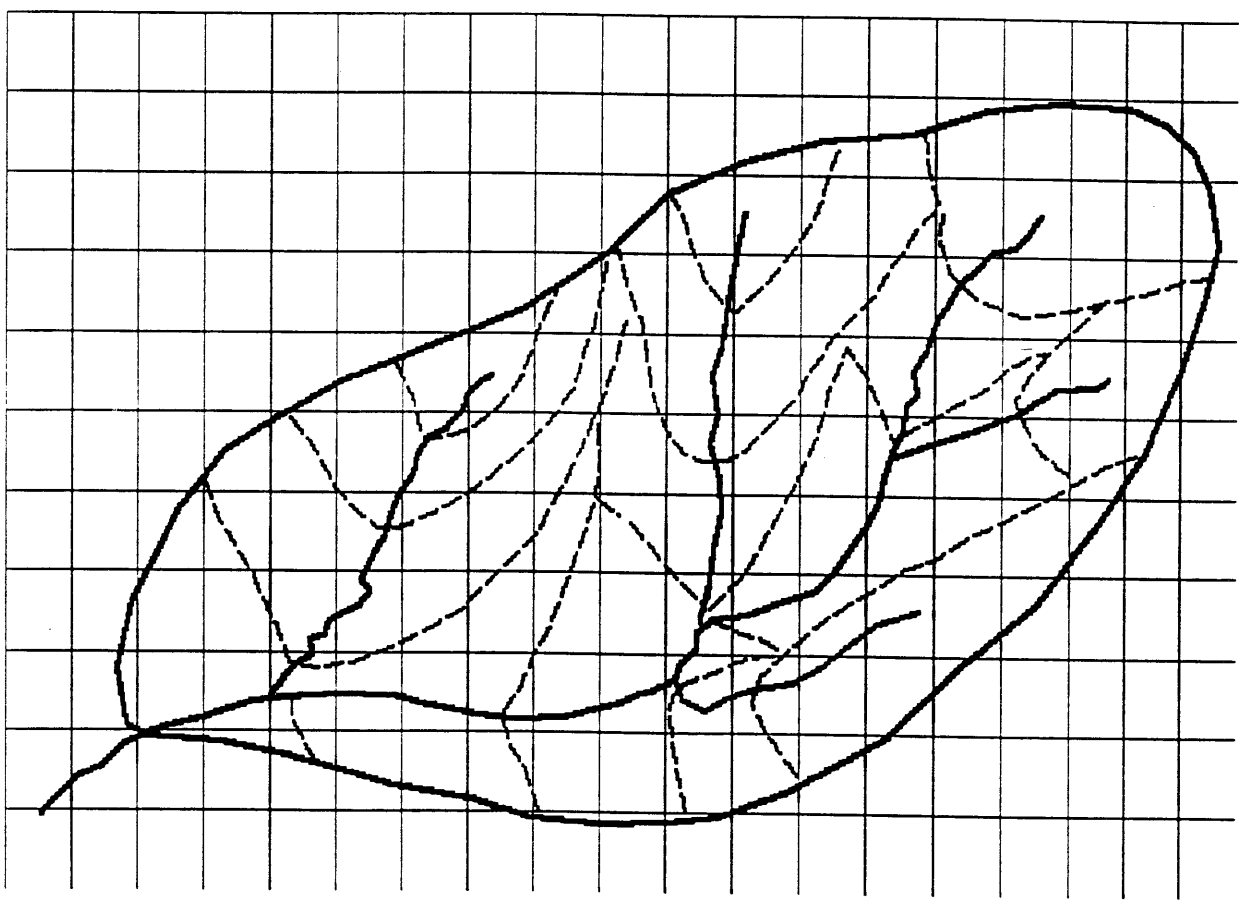

Fig. 3. 4 km x 4 km grid superimposed on threshold runoff (sub-basins)

6.3 Gridded Flash Flood Guidance

Almost all RFCs use the National Weather Service River Forecast System (NWSRFS) described by Anderson (1986) to simulate soil moisture conditions. This Operational Forecast System (OFS) uses observed precipitation (including the future WSR-88D precipitation estimates) and temperature to determine the mean areal precipitation and snowmelt over the forecast basins via the NWS Snow Accumulation and Ablation Temperature Index Model (SNOW-17) along with one of several rainfall-runoff models, e.g., Antecedent Precipitation Index (API) models, Sacramento Soil Moisture Accounting (SACSMA) model, and Xinanjiang model, which convert the precipitation and snowmelt to runoff.

Using forecast temperatures and any precipitation since the last state variable update along with the current forecast basin state variables, the snow model and the appropriate rainfall-runoff model will be used with several different precipitation values to compute the corresponding values of runoff. These define the rainfall-runoff curve for the basin. A rainfall-runoff curve must be determined for each rainfall duration (t_r) for which flash flood guidance is desired.

The gridded flash flood guidance is the rainfall needed to produce the gridded threshold runoff. This rainfall is interpolated from the appropriate rainfall-runoff curve at the threshold runoff value. The gridded flash flood guidance values then will be transmitted from an RFC database to a WFO where they will be automatically compared against the most recent gridded WSR-88D precipitation estimates as well as gridded quantitative precipitation forecasts (QPF). Based on this comparison, the WFO forecaster will decide if it is necessary to issue either a flash flood watch or warning.

References

1. Anderson, E.A. (1986). 'The National Weather Service River Forecast System and its application to cold regions,' 6th International Northern Research Symposium/Workshop, Michigan Technological University, Jan. 26-30, pp. 219-238.

2. Basco, D.R. (1987). 'Improved robustness of the NWS DAMBRK algorithm,' Hydraulic Engineering, (Proc. of the 1987 National Conference on Hydraulic Engineering), ASCE, New York, Aug., pp. 776-781.

3. Cunge, J.A. (1969). 'On the subject of a flood propagation computation method (Muskingum method),' J. Hydraul. Res., Vol. 7, No. 2, pp. 205-230.

4. Fread, D.L. (1974). Numerical Properties of Implicit Four-Point Finite Difference Equations of Unsteady Flow, HRL-45, NOAA Tech. Memo NWS HYDRO-18, Hydrologic Research Laboratory, National Weather Service, Silver Spring, Md., 38 pp.

5. Fread, D.L. (1977). 'The development and testing of a dam-break flood forecasting model,' Proc. of Dam-Break Flood Modeling Workshop, U.S. Water Resources Council, Washington, D.C., pp. 164-197.

6. Fread, D.L. (1978). 'NWS operational dynamic wave model,' Verification of Mathematical and Physical Models, Proceedings of 26th Annual Hydr. Div. Specialty Conf., ASCE, College Park, Md., pp. 455-464.

7. Fread, D.L. (1983). Applicability Criteria for Kinematic and Diffusion Routing Models, HRL-176, Hydrologic Research Laboratory, National Weather Service, Silver Spring, Md., 16 pp.

8. Fread, D.L. (1985). 'Channel routing,' Hydrological Forecasting, (Eds: M.G. Anderson and T.P. Burt), John Wiley and Sons, New York, Chapter 14, pp. 437-503.

9. Fread, D.L. (1988). The NWS DAMBRK Model: Theoretical Background/User Documentation, HRL-256, Hydrologic Research Laboratory, National Weather Service, Silver Spring, Md., 315 pp.

10. Fread, D.L. (1992). 'Numerical flood routing models used in NWS,' US/PRC Flood Forecasting Symposium/Workshop, Portland, Or., pp. 279-314.

11. Fread, D.L., and Lewis, J.M. (1988). 'FLDWAV: a generalized flood routing model,' Proc. of National Conference on Hydraulic Engineering, ASCE, Colorado Springs, Co., pp.668-673.

12. Fread, D.L., Lewis, J.M., and Wiele, S.M. (1991). The NWS Simplified Dam-Break Flood Forecasting Model, HRL-278, Hydrologic Research Laboratory, National Weather Service, Silver Spring, Md., 46 pp.

13. Jarrett, R.D. (1984). 'Hydraulics of high-gradient streams,' J. Hydraul. Div., ASCE, Vol. 110, No. HY11, Nov., pp. 1519-1539.

14. Jones, S.B. (1981). 'Choice of space and time steps in the Muskingum-Cunge flood routing method,' Proc. of Instn. Civil Engr., Part 2, No. 71, pp. 759-772.

15. Leenderste, J.J. (1967). 'Aspects of a computational model for long-period water wave propagation,' Rand Report RM-5294-PR, Rand Corp. Santa Monica, Cal., 165 pp.

16. Linsley, R.K., Kohler, M.A., and Paulhus, J.L.H. (1986). Hydrology for Engineers, McGraw-Hill, New York, pp. 502-530.

17. Samuels, P.G. (1985). Models of Open Channel Flow Using Preissmann's Scheme, Cambridge University, Cambridge, England, pp. 91-102.

18. Snyder, F.F. (1938). 'Synthetic unit hydrographs,' Trans. Am. Geophys. Union, Vol. 19, Pt. 1, pp. 447-454.

19. Sweeney, T. (1991). Modernized Areal Flash Flood Guidance, HRL-279, NOAA Tech. Memo NWS Hydro-44, Hydrologic Research Laboratory, National Weather Service, Silver Spring, Md., 30 pp.

20. Wetmore, J.N, and Fread, D.L. (1984). The NWS Simplified Dam Break Flood Forecasting Model for Desk-Top and Hand-Held Microcomputers, printed and distributed by the Federal Emergency Management Agency (FEMA), 47 pp.